Simulation of 200–400 MeV/u $^{12}C+^{12}C$ elastic scattering on SHARAQ spectrometer *

YU Lei(于蕾)[1] ZHANG Gao-Long(张高龙)[1;1)] S. Terashima[1] I. Tanihata[1,2] LE Xiao-Yun(乐小云)[1]

[1] School of Physics and Nuclear Energy Engineering, Beihang University, Beijing 100191, China
[2] Research Center for Nuclear Physics, Osaka University, Osaka 567-0047, Japan

Abstract: In order to further obtain the information of three-body force (TBF) from 200–400 MeV/u $^{12}C+^{12}C$ elastic scattering, we plan to perform this experiment on a SHARAQ spectrometer. Based on the experimental condition of the Radioactive Ion Beam Factory (RIBF)-SHARAQ facility, a simulation is given to find a compromise between the better energy and angular resolutions, and higher yield by optimizing the target thickness, beam transport mode, beam intensity and angular step. From the simulation, we found that the beam quality mainly limits the improvements of energy and angular resolutions. A beam tracking system as well as a lateral and angular dispersion-matching technique are adopted to reduce the influence of beam quality. According to the two angular settings of SHARAQ as well as the expected cross sections on the basis of the theoretical model, the energy and angular resolutions, and statistical accuracy are estimated.

Key words: elastic scattering, three-body force, SHARAQ, Monte Carlo method

PACS: 02.70.Uu, 21.30.-x, 25.70.Bc **DOI:** 10.1088/1674-1137/39/2/026201

1 Introduction

The understanding of the interaction between composite nuclei is one of the key issues in studying various nuclear reactions. Elastic scattering, which is one of the nuclear reactions, is well described by the optical model. Generally the optical potential in the low energy region has an attractive real part together with an absorptive imaginary part. However, the optical potential depends on the incident energy. High energy deuteron scattering showed an attractive-to-repulsive transition of optical potential [1]. Besides this, there is no such study about the attractive-to-repulsive transition of the optical potential on the theoretical and experimental parts of the scattering of composite projectiles. Recently, Furumoto et al calculated the optical potential of composite projectiles on the basis of the complex G-matrix. The calculated double-folding model potential revealed the attractive-to-repulsive transition of the real part of the optical potential with the increase of incident energies [2]. It is found that the angular distribution of $^{12}C+^{12}C$ elastic scattering shows a strong diffractive oscillation pattern at 300 MeV/u with a three-body force (TBF) effect and at 400 MeV/u without a TBF effect, respectively. However, at 200 MeV/u with and without TBF there is no such strong diffractive oscillation. So the TBF effect can be explored from the angular distribution of 200–400 MeV/u $^{12}C+^{12}C$ elastic scattering. Meanwhile, when considering the effect of the coupling channel [3], the inelastic scattering should be measured. As a result, in one laboratory we require not only a 200–400 MeV/u ^{12}C beam but also a spectrometer with high energy resolution. So we prepare the experiment of 200–400 MeV/u $^{12}C+^{12}C$ scattering on the Radioactive Ion Beam Factory (RIBF) beam line by using the magnetic spectrometer 'SHARAQ' at RIKEN in Japan.

The SHARAQ spectrometer is a high resolution spectrometer. It has a good angular resolution in not only horizontal but also vertical directions, which is a great advantage for high energy heavy-ion scattering in order to precisely determine the scattering angle at the forward region. Its design parameters are described in [4]. In this experiment the elastic and inelastic channels need to be separated while the diffraction pattern of the angular distribution is required to take measurements precisely, thus the high energy and angular resolutions are desired. For this purpose we need to optimize the target thickness, beam intensity, beam transport mode and angular step, etc. So we use the Monte Carlo method to simulate these procedures [5]. It will provide a good support for the experimental design. Then during the experiment the SHARAQ spectrometer can clearly separate elastic

Received 1 April 2014
* Supported by National Nature Science Foundation of China (11035007, 11235002, 11175011)
1) E-mail: zgl@buaa.edu.cn

and inelastic channels. The final experimental data will provide decisive evidence for the repulsive nature of the heavy-ion optical potential and the TBF effect, as well as information about the energy region where the attractive to repulsive transition occurs.

2 Simulation process

The main experimental conditions in our simulation are indicated in Table 1. The most severe restrictions for $^{12}C+^{12}C$ experiment are the energy and angular resolutions as well as production yield. First, beam momentum spread and beam emittance, which are determined by the beam facility, will directly affect the energy and angular resolutions. To obtain better energy and angular resolutions, the thinner target is preferred to reduce the multiple Coulomb scattering. However, the yield is decreased. In addition, low beam intensity can be helpful for the beam tracking operation. However, adequate statistical information is required. Therefore, a compromise should be made among these requirements [6]. On the premise that enough statistical information is provided, the principle of our simulation is to achieve a good energy and angular resolution by optimizing the target thickness, beam transport mode, beam intensity and angular step. In this section, these parameters are described in detail.

Table 1. The experimental condition in the RIBF-SHARAQ facility.

experimental condition	assumed value
beam emittance	3 mm·mrad in σ
beam intensity	up to 10^7/s
beam momentum spread	0.05% in σ
position resolution of focal plane detector	100 μm in σ
angular resolution of focal plane detector	0.2 mrad in σ
trigger rate	500 Hz

To know how these factors affect the energy and angular resolutions, there are two procedures to be considered. First, the position $X_{\rm f}$ and angle $\theta_{\rm f}$ of the scattered particles are calculated at the focal plane (FP) of the spectrometer by Eqs (1) and (2). Then we can deduce the scattering angle $\theta_{\rm 3m}$ and momentum $P_{\rm m}$ of scattered carbon from the target by using Eqs (3)–(5).

$$\theta_{\rm f} = \langle\theta|x\rangle X_0+\langle\theta|\theta\rangle(\theta_3-\theta_{\rm C}-\theta_0+\theta_{\rm M.S.}) +\langle\theta|\delta p\rangle\frac{\delta P}{P}+\langle detector\rangle_\theta, \quad (1)$$

$$X_{\rm f} = \langle x|x\rangle X_0+\langle x|\delta p\rangle\frac{\delta P}{P}+\langle detector\rangle_x, \quad (2)$$

$$\frac{\delta P_{\rm m}}{P} = \frac{X_{\rm f}}{\langle x|\delta p\rangle}, \quad (3)$$

$$\begin{aligned}\theta_{\rm 3m} &= \theta_{\rm C}+\left(\theta_{\rm f}-\frac{\langle\theta|\delta p\rangle}{\langle x|\delta p\rangle}\cdot X_{\rm f}\right)/\langle\theta|\theta\rangle \\ &= \theta_3-\theta_0+\theta_{\rm M.S.}+(\langle\theta|x\rangle X_0+\langle detector\rangle_\theta)/\langle\theta|\theta\rangle \\ &\quad -\frac{\langle\theta|\delta p\rangle}{\langle\theta|\theta\rangle}\left(\frac{\langle x|x\rangle X_0}{\langle x|\delta p\rangle}+\frac{\langle detector\rangle_x}{\langle x|\delta p\rangle}\right), \end{aligned} \quad (4)$$

$$\begin{aligned}P_{\rm m} &= P_0\left(1+\frac{\delta P_{\rm m}}{P}\right) \\ &= P_0\left(1+\frac{\langle x|x\rangle X_0}{\langle x|\delta p\rangle}+\frac{\delta P}{P}+\frac{\langle detector\rangle_x}{\langle x|\delta p\rangle}\right),\end{aligned} \quad (5)$$

here X_0, θ_0 are the beam position and angle before the target, respectively. θ_3 and $\theta_{\rm C}$ are the real scattering angles from the target and the setting central angle of the spectrometer, respectively. $\frac{\delta P}{P}$ is the offset factor for the central momentum P_0. $\langle detector\rangle_x$ and $\langle detector\rangle_\theta$ are the position and angular resolutions of the FP detector, respectively. $\theta_{\rm M.S.}$ is the deflection angle through multiple scattering in the target. The components of the angle brackets denote the matrix elements of SHARAQ.

Equations (3)–(5) illustrate that the beam emittance (X_0, θ_0), multiple scattering effect and resolutions of the FP detector ($\langle detector\rangle_x$, $\langle detector\rangle_\theta$) have an influence on the resolution of the measured scattering angle, while the energy resolution is affected by the momentum spread ($\frac{\delta P}{P}$), X_0 and $\langle detector\rangle_x$. From our calculation, the beam quality (emittance and momentum spread), which is a designed parameter of the beam facility, becomes a dominant factor limiting the angular and energy resolutions. Therefore, on one hand, the $\theta_{\rm M.S.}$ should be as small as possible to improve the angular resolution. The angular distribution of multiple Coulomb scattering is roughly Gaussian distribution with a width given by [7, 8],

$$\sigma_{\rm M.S.}=\frac{13.6\ {\rm MeV}}{\beta cp}z\sqrt{x/X_0}\left[1+0.038\ln\left(\frac{x}{X_0}\right)\right]\,[{\rm rad}], \quad (6)$$

here p, βc, and z are the momentum, velocity, and charge number of the incident particles, respectively. x/X_0 is the thickness of the scattering medium in radiation lengths. For 100 mg/cm^2 ^{12}C target, $\sigma_{\rm M.S.}$ is about 1.33 mrad (much less than emittance). On the other hand, the energy straggling caused by multiple scattering increases the momentum spread after the target, and then the energy resolution deteriorates. As a result, the thinner target is preferred to reduce the multiple scattering effect.

Considering the effect of the beam quality, it is necessary to use beam tracking to observe the beam trajectory and momentum before the target. The higher angular and energy resolutions can be expected using this information. However, the beam intensity must be kept under 10^5/s for proper detector operation [9], otherwise it leads to lower yield. Another solution for keeping the energy resolution is to use lateral and angular dispersion-matching optics, which can compensate the momentum spread. But the angular resolution will remain bad without beam tracking. In a word, the beam intensity, beam transport mode and production yield should be considered to find a compromise.

The yield can be estimated as follows

$$\mathrm{d}N' = \frac{\mathrm{d}\sigma}{\mathrm{d}\Omega} \times I \times N_{\mathrm{S}} \times \mathrm{d}\Omega, \tag{7}$$

where $\mathrm{d}N'$ is the number of events, $\frac{\mathrm{d}\sigma}{\mathrm{d}\Omega}$ is the differential cross section of ^{12}C+^{12}C elastic scattering. I and N_{S} are the beam intensity and the number of target per square, respectively. $\mathrm{d}\Omega$ is the solid angle. The theoretical cross sections of 200–400 MeV/u ^{12}C+^{12}C elastic scattering are estimated by FRESCO program. To obtain higher yield, the higher beam intensity, the thicker target and the larger acceptance of the solid angle are needed. Beam intensity and target thickness have already been discussed. The solid angle is calculated according to the angular step and vertical acceptance of SHARAQ. The angular step is determined by angular resolution. The larger solid angle means the worse angular resolution. Meanwhile, the yield should be limited considering the typical trigger rate (500/s) of the data acquisition system. Therefore, a balance needs to be found between the beam intensity, target thickness, angular resolution and yield.

3 Results and discussions

To achieve the compromise between the angular and energy resolutions as well as the production yield, we decide to give the two angular settings of SHARAQ which are shown in Table 2.

Table 2. The setting parameters of SHARAQ spectrometer for 200–400 MeV/u ^{12}C+^{12}C elastic scattering.

	Set 1	Set 2
angular region	2.4°±1.7°	3.5°±0.9°
target thickness	30 mg/cm^2	100 mg/cm^2
beam intensity	10^5/s (beam tracking)	10^7/s
transport mode	achromatic mode	dispersive mode
angular step	0.3°	0.7°

Our interesting angular range is 1.0°–4.0°. The horizontal acceptances of SHARAQ in achromatic mode and dispersion-matching mode are ±30 mrad (1.7°) and ±17 mrad (0.9°), respectively. To avoid the incident beam directly entering the FP detector, the most forward angle of the spectrometer has to be larger than 0.7° which corresponds to 4 σ of the angular spread of the beam (3 mrad in σ). So the central angle of Set 1 is designed as 2.4°. Set 1 covers the main interesting angular region, and Set 2, which is designed as 3.5°±0.9°, is used for correction. Fig. 1 shows a schematic view of angular acceptances of two different angular settings. The target thicknesses 30 mg/cm^2 and 100 mg/cm^2 are selected through the overall consideration of beam intensity, multiple Coulomb scattering, yield and total trigger rate.

For Set 1 we use the achromatic beam transport mode to the target with the beam tracking system. The expected tracking resolutions of position, angle and momentum on the target are 0.3 mm, 0.5 mrad, and 0.02% in σ, respectively. By substituting those values into Eq. (4), the angular resolution better than 1 mrad is achieved. The improvement is far better than that without beam tracking. The excitation energy spectra including ground and the first excited states of ^{12}C are illustrated in Fig. 2 for 200–400 MeV/u ^{12}C+^{12}C scattering to show the energy resolution in Set 1. We can see that the two states can be clearly separated at 200 MeV/u and 300 MeV/u. At 400 MeV/u incident energy it is no clearer than those at 200 MeV/u and 300 MeV/u. However, two peaks can be evidently observed. As a result, a good fitting can be used to distinguish them.

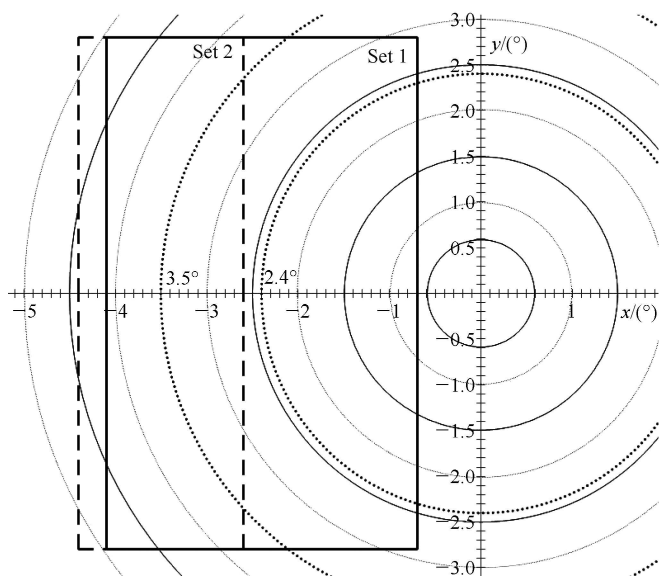

Fig. 1. Two different angular acceptances and the zenith angles with 0.5° step. Here the center of the circles is the beam position. Solid and dashed squares are angular acceptances of Set 1 and Set 2, respectively.

Set 2 uses a dispersive mode with lateral and angular dispersion-matching optics. The better energy resolution could be expected than that in Set 1. A higher beam intensity up to 10^7/s is used to compensate the lower cross section in this region. On the other hand, angular resolu-

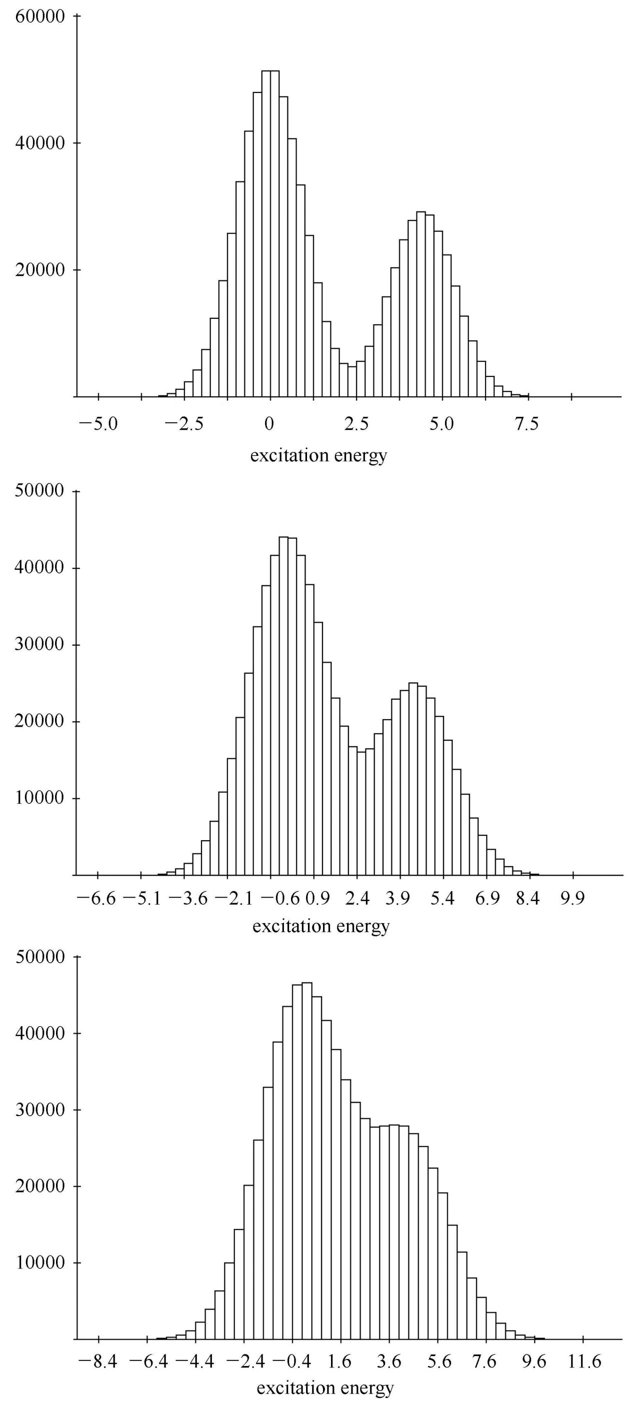

Fig. 2. The excitation energy spectra of ^{12}C+^{12}C elastic at 200 MeV/u (upper), 300 MeV/u (middle) and 400 MeV/u (lower) including the ground and the first excited (4.44 MeV) states in Set 1.

tion is assumed 3 mrad in σ due to the worse beam emittance. But it is enough for the purpose of data check.

The theoretical and expected angular distributions of ^{12}C+^{12}C elastic scattering at 200, 300 and 400 MeV/u are shown in Fig. 3. Both settings have enough overlap region with different angular resolutions. At the forward angle setting, we can observe a clear diffraction pattern with 0.3° angular step. When keeping the statistical error 3% at around 2°, the beam time of 20 h is required for each energy. At a backward angle setting, from 3° to 4° region 0.7° angular step is used. When keeping the statistical error 3%, the beam time is 10 h at each energy. After considering changing the incident energy, background measurement and detector setting, the total beam time is about 120 h (5 days).

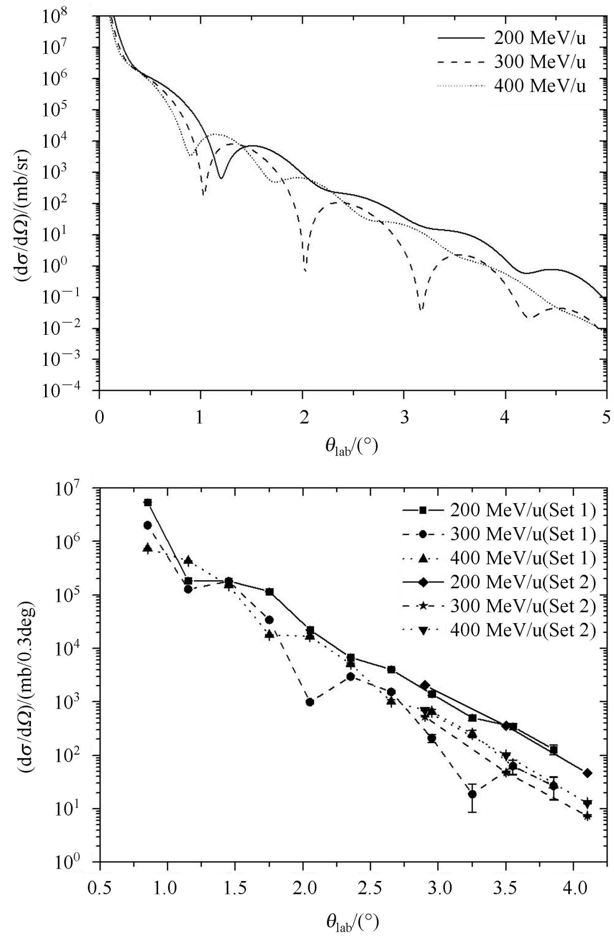

Fig. 3. Upper: Theoretical results of the angular distribution of ^{12}C+^{12}C elastic scattering at 200, 300 and 400 MeV/u on the basis of global potential. Lower: The expected angular distribution in frame of expected statistical errors at 200, 300 and 400 MeV/u incident energies. 0.3° and 0.7° angular steps for forward and backward angle settings, respectively.

4 Summary

In order to obtain the good energy and angular resolutions as well as high production yield for the 200–400 MeV/u ^{12}C+^{12}C elastic scattering experiment, we use the Monte Carlo method to simulate the kinematic process based on the experimental condition in the RIKEN-SHARAQ facility. After taking into account target thickness, beam intensity, beam transport mode, detector resolution and so on, the two angular settings are designed. Set 1 uses an achromatic beam transport mode with beam tracking. The ground state of ^{12}C can be clearly distinguished from the first excited state. Set 2 utilizes a dispersive mode with a lateral and angular dispersion matching technique. Total beam time and expected cross sections are also estimated.

In this experiment, there are not many new detectors or techniques involved. After software simulation some hardware conditions, such as beam monitor, beam stopper, high voltage optimization and background product, need to be considered to achieve the expected results.

References

1 Van Sen N, Yanlin Y, Arvieux J, Gaillard G. Nucl. Phys. A, 1987, **464**(4): 717

2 Furumoto T, Sakuragi Y, Yamamoto Y. Phys. Rev. C, 2010, **82**: 044612

3 Furumoto T, Sakuragi Y. Phys. Rev. C, 2013, **87**: 014618

4 Uesaka T, Shimoura S, Sakai H, Berg G P A, Nakanishi K, Sasamoto Y, Saito A, Michimasa S, Kawabata T, Kubo T. Nucl. Instrum. Methods Phys. Res. B, 2008, **266**: 4218

5 GUO C L, ZHANG G L, Tanihata I, LE X Y. Chin. Phys. C, 2012, **36**(3): 205

6 Yoshiko S Study of the isovector non-spin-flip monopole resonance via the super-allowed Fermi type charge exchange (^{10}C, ^{10}Bγ) reaction PhD Thesis University of Tokyo, Japan; ed O. Hideaki et al Nuclear Structure Problems-Proceedings of the French-Japanese Symposium (Singapore: World Scientific) ISBN♯ 9789814417952 2013 148–151

7 Highland V L. Nucl. Instrum. Methods, 1975, **129**: 497; Nucl. Instrum. Methods, 1979, **161**: 171

8 Lynch G R, Dahl O I. Nucl. Instrum. Methods B, 1991, **58**: 6

9 Kenjiro M. Study of the isovector spin monopole resonance via the (t, ^{3}He) reactions at 300 MeV/u (PhD Thesis). University of Tokyo, Japan; Progress of Theoretical Physics Supplement, 2012, **196**: 150